




Solvothermal syntheses and characterizations of polysulfido-thioantimonate and thioantimonate templated by Co-phen complex cation

Yun Liu, Jialin Lu, Fang Wang, Yali Shen, Chunying Tang, Yong Zhang & Dingxian Jia

To cite this article: Yun Liu, Jialin Lu, Fang Wang, Yali Shen, Chunying Tang, Yong Zhang & Dingxian Jia (2015) Solvothermal syntheses and characterizations of polysulfido-thioantimonate and thioantimonate templated by Co-phen complex cation, Journal of Coordination Chemistry, 68:13, 2334-2346, DOI: [10.1080/00958972.2015.1045500](https://doi.org/10.1080/00958972.2015.1045500)

To link to this article: <http://dx.doi.org/10.1080/00958972.2015.1045500>

 View supplementary material 

 Accepted author version posted online: 27 Apr 2015.
Published online: 20 May 2015.

 Submit your article to this journal 

 Article views: 50

 View related articles 

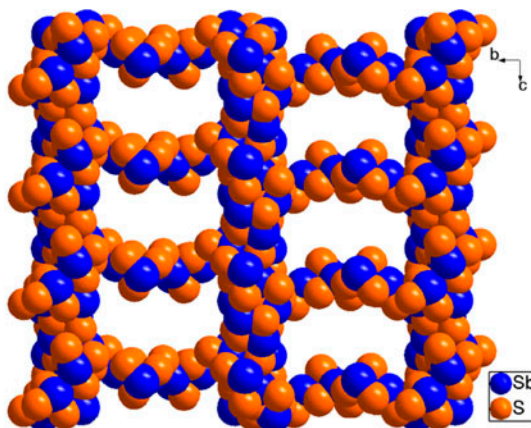
 View Crossmark data 

Solvothermal syntheses and characterizations of polysulfido-thioantimonate and thioantimonate templated by Co-phen complex cation

YUN LIU, JIALIN LU, FANG WANG, YALI SHEN, CHUNYING TANG,
YONG ZHANG and DINGXIAN JIA*

College of Chemistry, Chemical Engineering and Materials Science, Soochow University, Suzhou, PR China

(Received 11 September 2014; accepted 7 April 2015)



Polythioantimonate $[\text{Co}(\text{phen})_3][\text{Sb}_4\text{S}_5(\text{S}_4)_2]$ (**1**), thioantimonates $[\text{Co}(\text{phen})_3]_2\text{Sb}_{18}\text{S}_{29}$ (**2**), and $[\text{H}_3\text{O}][\text{Co}(\text{phen})_3]\text{SbS}_4 \cdot 9\text{H}_2\text{O}$ (**3**) were solvothermally prepared using $[\text{Co}(\text{phen})_3]^{2+}$ as a structure directing agent in different protic solvents, indicating solvent effects on the solvothermal system of Co/Sb/S/phen.

Polysulfido-thioantimonate $[\text{Co}(\text{phen})_3][\text{Sb}_4\text{S}_5(\text{S}_4)_2]$ (**1**), thioantimonates $[\text{Co}(\text{phen})_3]_2\text{Sb}_{18}\text{S}_{29}$ (**2**), and $[\text{H}_3\text{O}][\text{Co}(\text{phen})_3]\text{SbS}_4 \cdot 9\text{H}_2\text{O}$ (**3**) (phen = 1,10-phenanthroline) were prepared using $[\text{Co}(\text{phen})_3]^{2+}$ formed *in situ* as a structure directing agent in 80 and 50% CH_3OH aqueous solution or water solution, respectively. In **1**, eight Sb^{3+} ions are connected by ten $\mu\text{-S}^{2-}$ and four $\mu\text{-S}_4^{2-}$ bridging ligands to form a circular polysulfide thioantimonate anion $[\text{Sb}_8\text{S}_{10}(\text{S}_4)_4]^{4-}$ which contains a sixteen-membered Sb_8S_8 heteroring. The Sb^{3+} ions are in trigonal pyramidal SbS_3 or trigonal bipyramidal $\psi\text{-SbS}_4$ geometries. In **2**, sixteen SbS_3 and two $\psi\text{-SbS}_4$ units are interconnected by sharing S atoms to form a 3-D $[\text{Sb}_{18}\text{S}_{29}^{4-}]_{\infty}$ framework containing an interpenetrating channel system, in which the $[\text{Co}(\text{phen})_3]^{2+}$ complexes are enclosed. In **3**, by $\text{O-H}\cdots\text{O}$ and $\text{O-H}\cdots\text{S}$ H-bonding,

*Corresponding author. Email: jjadingxian@suda.edu.cn

$[\text{SbS}_4]^{3-} \cdot \text{H}_2\text{O}$ and H_3O^+ are interconnected into a $\{\text{H}_3\text{O}-\text{SbS}_4-(\text{H}_2\text{O}_9)\}_n^{2n-}$ anionic layer, which contains a $(\text{H}_2\text{O})_6$ water cluster. The $[\text{Co}(\text{phen})_3]^{2+}$ complexes are located between the layers. The syntheses of 1–3 show the influences of different solvents on the Co/Sb/S/phen system. The optical band gaps of 1–3 are 2.02, 2.11, and 2.27 eV, respectively.

keywords: Thioantimonate; Cobalt; Solvothermal syntheses; Solvent effect

1. Introduction

Chalcogenidoantimonates attract attention because of their structural diversity and interesting optical and electrical properties [1, 2]. Effort in templating syntheses in coordinative ethylene polyamines under solvothermal conditions has led to numerous chalcogenidoantimonates containing transition metal (TM) complexes as charge compensating counterions or structural components. The solvothermal system Sb/S/TM has been extensively investigated in a variety of ethylene polyamines, such as ethylenediamine (en) [2(a), 3], diethylenetriamine (dien) [4], tris(2-aminoethyl)amine (tren) [5] and triethylenetetramine (trien) [6], or mixed ethylene polyamines [5(g), 7]. The TM^{n+} ions are coordinated to polyamines to form chelating complex cations, which act as templates or structure directing agents in the syntheses. The structures and denticities of the ethylene polyamines influence the structures and compositions of the final thioantimonates, giving $[\text{Co}(\text{en})_3]\text{CoSb}_4\text{S}_8$ [2(a)] and $\{[\text{Co}(\text{tren})]_2[\text{CoSb}_2\text{S}_6]\} \cdot \text{H}_2\text{O}$ [5(g)], for example. The former, which was prepared with bidentate en, contains a free $[\text{Co}(\text{en})_3]^{2+}$ counter cation, while the latter with tridentate tren contains a $[\text{Co}(\text{tren})]^{2+}$ fragment coordinated by an inorganic $[\text{CoSb}_2\text{S}_6]^{4-}$ anion. Particularly, in the case of thiophilic TM ions (such as Cu^+ and Ag^+), the thiophilic TM ions are easily incorporated into the binary Sb/S composition to form ternary thioantimonates with protonated amines as the charge compensating cations [8, 9]. On the other hand, the structures and compositions of the TM-containing thioantimonates are sensitive to the solvothermal reaction conditions. Examples to exhibit the influence of solvothermal reaction conditions are the Ni-thioantimonates prepared from the Ni/Sb/S system in the presence of the same polyamine dien. Seven Ni-thioantimonates, $[\text{Ni}(\text{dien})_2]_3(\text{SbS}_4)_2$ [4(a)], $[\text{Ni}(\text{dien})_2]_9\text{Sb}_{22}\text{S}_{42} \cdot 0.5\text{H}_2\text{O}$ [4(b)], $[\text{Ni}(\text{dien})_2]_2\text{Sb}_4\text{S}_8$ [4(c)], $[\text{Ni}(\text{dien})_2]_2\text{Sb}_4\text{S}_9$ [4(d)], $[\text{Ni}(\text{dien})_2]\text{Sb}_4\text{S}_7 \cdot \text{H}_2\text{O}$, $[\text{Ni}(\text{dien})_2]_3\text{Sb}_{12}\text{S}_{21} \cdot \text{H}_2\text{O}$ [4(e)], and $[\text{Ni}(\text{dien})_2]_3(\text{Sb}_3\text{S}_6)_2$ [4(f)] were prepared using the same starting materials, but with different molar ratio of reactants, in different solvents, or at different temperature. Solvothermal syntheses in the Sb/S/TM/polyamine system usually produce thioantimonates(III) [4–7]. The thioantimonates(V) are seldom obtained, and the limited examples include $[\text{Ni}(\text{dien})_2]_3(\text{SbS}_4)_2$ [4(a)], $[\text{Co}(\text{dien})_2][\text{Co}(\text{tren})\text{SbS}_4]_2 \cdot 0.5\text{H}_2\text{O}$ [5(g)], $[\text{Cr}(\text{en})_3]\text{SbS}_4$ [10], $[\text{Mn}(\text{tren})(\text{Htren})]\text{SbS}_4$ [11], and $[\text{Ni}(\text{en})_3]_2(\text{SbS}_4)(\text{NO}_3)$ [12]. Thioantimonates(V) other than thioantimonates(III) were obtained in similar solvothermal syntheses with TM being replaced by lanthanide (Ln), giving $[\text{Ln}(\text{dien})_2(\mu-\eta^1, \eta^2-\text{SbS}_4)]_n$ (Ln = Pr, Nd, Sm) and $[\text{Ln}(\text{dien})_2(\eta^2-\text{SbS}_4)]$ (Ln = Eu, Dy), for example [13]. The only example of thioantimonates(III) containing a Ln complex is $[\text{La}(\text{dien})_2(\mu_4-\text{Sb}_2\text{S}_5)(\mu_3-\text{SO}_4)]_n$ [14].

Compared with the TM-containing thioantimonates with aliphatic polyamines, the compounds containing TM complexes with aromatic ligands are less explored [15]. In our previous work, we prepared polyselenidoarsenates and selenidoarsenates using the TM complexes of phen as structure directing agents and found that the TM-phen complexes show different structure directing effects from the TM-aliphatic-amine complexes in the

solvothermal syntheses of selenidoarsenates [16]. In order to explore the effects of TM-phen complexes and solvents on the solvothermal syntheses of thioantimonates, the Co/Sb/S/phen system was investigated in H₂O and mixed CH₃OH-H₂O solvents, and a polysulfido-thioantimonate(III) [Co(phen)₃][Sb₄S₅(S₄)₂] (**1**), a thioantimonate(III) [Co(phen)₃]₂Sb₁₈S₂₉ (**2**), and a thioantimonate(V) [H₃O][Co(phen)₃]₂SbS₄·9H₂O (**3**) were prepared.

2. Experimental

2.1. Materials and physical measurements

All starting chemicals were of analytical grade and used as received. Elemental analyses were conducted using an EA1110-CHNS-O elemental analyzer. Fourier transform infrared (FT-IR) spectra were recorded using a Nicolet Magna-IR 550 spectrometer on dry KBr disks from 4000 to 400 cm⁻¹. Powder X-ray diffraction (PXRD) patterns were collected on a D/MAX-3C diffractometer using graphite monochromated Cu K α radiation ($\lambda = 1.5406 \text{ \AA}$). Energy dispersive X-ray measurements were performed on a scanning electron microscope Hitachi S-4700. Room temperature optical diffuse reflectance spectra of powder samples were obtained using a Shimadzu UV-3150 spectrometer. Absorption (α/S) data were calculated from the reflectance using the Kubelka-Munk function $\alpha/S = (1 - R)^2/2R$ [17].

2.2. Synthesis of the complexes

2.2.1. [Co(phen)₃][Sb₄S₅(S₄)₂] (1**).** CoCl₂·6H₂O (48 mg, 0.2 mmol), phen·H₂O (119 mg, 0.6 mmol), Sb (73 mg, 0.6 mmol), S (58 mg, 1.8 mmol), and dien (116 mg, 1.13 mmol) were dispersed in 3 mL of CH₃OH aqueous solution (80% in H₂O) by stirring, and the dispersion was loaded into a polytetrafluoroethylene (PTFE) lined stainless steel autoclave of volume of 10 mL. The sealed autoclave was heated to 140 °C for 6 days and then cooled to ambient temperature. The resulting product contained dark-red crystals of **1** and some black powder. The crude product was transferred into a vial which was filled with water. Most of the black powder was suspended in water, which was then decanted leaving behind crystals. This procedure was repeated until the water remained clear. The red crystals of **1** were collected by filtering, washed with methanol, and stored under vacuum (yield: 104 mg, 46% based on Sb). Elemental analysis results of the crystals are consistent with the stoichiometry of C₃₆H₂₄N₆CoSb₄S₁₃. Anal. Calcd for C₃₆H₂₄N₆CoSb₄S₁₃ (%): C, 28.76; H, 1.61; N, 5.59. Found: C, 28.65; H, 1.55; N, 5.48. IR data (KBr, cm⁻¹): 3801 (w), 3741 (w), 3045 (w), 2353 (w), 1666 (s), 1582 (w), 1513 (s), 1422 (s), 1380 (w), 1341 (w), 1217 (w), 1142 (w), 1095 (m), 954 (w), 843 (s), 772 (m), 726 (s), 665 (w), 502 (m), 447 (w), 423 (m).

2.2.2. [Co(phen)₃]₂[Sb₁₈S₂₉] (2**).** CoCl₂·6H₂O (48 mg, 0.2 mmol), phen·H₂O (119 mg, 0.6 mmol), Sb (73 mg, 0.6 mmol), S (58 mg, 1.8 mmol), and dien (105 mg, 1.02 mmol) were dispersed in 3 mL of CH₃OH aqueous solution (50% in H₂O) by stirring, and the dispersion was loaded into a 10 mL PTFE lined stainless steel autoclave. The sealed autoclave was heated to 140 °C for six days and then cooled to ambient temperature. The resulting product contained red crystals of **2** and some black powder. The crude product was handled

by the same purification process as that of **1** and red crystals of **2** were obtained (yield: 75 mg, 52% based on Sb). Elemental analysis results of the crystals are consistent with the stoichiometry of $C_{72}H_{48}N_{12}Co_2Sb_{18}S_{29}$. Anal. Calcd for $C_{72}H_{48}N_{12}Co_2Sb_{18}S_{29}$ (%): C, 20.02; H, 1.12; N, 3.89. Found: C, 19.89; H, 0.98; N, 3.77. IR data (KBr, cm^{-1}): 3732 (w), 3041 (w), 2365 (m), 1511 (s), 1429 (m), 1336 (w), 1141 (w), 1100 (w), 981 (s), 855 (s), 779 (s), 720 (vs), 665 (m), 604 (w), 555 (w), 549 (w), 422 (s).

2.2.3. $[H_3O][Co(phen)_3]SbS_4 \cdot 9H_2O$ (3**).** $CoCl_2 \cdot 6H_2O$ (95 mg, 0.4 mmol), $phen \cdot H_2O$ (238 mg, 1.2 mmol), Sb (49 mg, 0.4 mmol), S (38 mg, 1.2 mmol), and dien (124 mg, 1.20 mmol) were dispersed in 3 mL of H_2O by stirring, and the dispersion was loaded into a 10 mL PTFE lined stainless steel autoclave. The sealed autoclave was heated to 160 °C for six days and then cooled to ambient temperature. The resulting product was handled by the same purification process as that of **1** and yellow prism crystals of **3** were obtained (yield: 227 mg, 55% based on Sb). Elemental analysis results of the crystals are consistent with the stoichiometry of $C_{36}H_{45}N_6O_{10}CoSbS_4$. Anal. Calcd for $C_{36}H_{45}N_6O_{10}CoSbS_4$ (%): C, 41.95; H, 4.40; N, 8.15. Found: C, 41.76; H, 4.34; N, 8.02. IR data (KBr, cm^{-1}): 3930 (w), 3901(m), 3868 (m), 3836 (s), 3741 (s), 3675 (m), 3655 (m), 3618 (s), 3565 (w), 2982 (w), 1867 (w), 1834 (w), 1744 (m), 1698 (s), 1645 (m), 1518 (s), 1465 (m), 1432 (w), 1395 (w), 1337 (w), 1264 (w), 1153 (w), 1005 (w), 862 (w), 751 (m), 701 (m), 546 (w), 500 (m).

2.3. X-ray structure determination

Data were collected on a Rigaku Saturn CCD diffractometer at 293(2) K using graphite-monochromated Mo- $K\alpha$ radiation ($\lambda = 0.71073 \text{ \AA}$) to a maximum 2θ value of 50.70° . The intensity data sets were collected with a ω -scan method and reduced with the CrystalClear program [18]. An empirical absorption correction was applied for **1–3** using the multiscan method. Structures were solved with direct methods using SHELXS-97 [19] and refinement was performed against F^2 using SHELXL-97 [20]. All non-hydrogen atoms were refined anisotropically. Hydrogens were added geometrically and refined using the riding model. The O–H hydrogens in **3** were located in difference map, and were refined using a riding model. Technical details of data acquisition and selected refinement results are summarized in table 1.

3. Results and discussion

3.1. Syntheses

Title compounds were prepared in CH_3OH-H_2O or H_2O solvents under solvothermal conditions. The reaction of $CoCl_2 \cdot 6H_2O$, Sb, S, dien, and phen in 80% CH_3OH aqueous solution at 140 °C produced a cobalt polysulfido-thioantimonate(III) $[Co(phen)_3][Sb_4S_5(S_4)_2]$ (**1**). The reaction in 50% CH_3OH solutions afforded a cobalt thioantimonate(III) $[Co(phen)_3]_2Sb_{18}S_{29}$ (**2**). A thioantimonate (V) compound $[H_3O][Co(phen)_3]SbS_4 \cdot 9H_2O$ (**3**) was obtained by the reaction in water at 160 °C. The experimental PXRD patterns of the bulk phase for **1–3** are similar to the simulated PXRD pattern on the basis of single-crystal

Table 1. Crystallographic data and structure refinement details for 1–3.

	1	2	3
CCDC deposit no.	CCDC-1018727	CCDC-1018728	CCDC-1018751
Formula	C ₃₆ H ₂₄ N ₆ CoS ₁₃ Sb ₄	C ₇₂ H ₄₈ N ₁₂ Co ₂ S ₂₉ Sb ₁₈	C ₃₆ H ₄₅ N ₆ O ₁₀ CoS ₄ Sb
Formula mass	1503.32	4320.32	1030.70
Crystal system	Triclinic	Monoclinic	Triclinic
Space group	<i>P</i> -1	<i>P</i> 2 ₁	<i>P</i> -1
λ (Mo-K α) (Å)	0.71073	0.71073	0.71073
<i>a</i> (Å)	12.3411(15)	11.156(10)	12.1297(5)
<i>b</i> (Å)	13.5453(17)	41.25(2)	14.9167(6)
<i>c</i> (Å)	15.6587(17)	12.354(11)	15.1183(6)
α (°)	101.977(2)	90	117.748(5)
β (°)	95.423(2)	106.595	107.508(6)
γ (°)	113.406(2)	90	97.404(8)
<i>V</i> (Å ³)	3625.5(13)	5449(9)	2188.38(15)
<i>Z</i>	2	2	2
<i>D</i> _{calcd} (g cm ⁻³)	2.167	2.633	1.564
<i>F</i> (0 0 0)	1442	4000	1050
Reflections collected	22,692	24,543	17,787
Independent reflections	8370	10,030	7969
<i>R</i> _{int}	0.0382	0.0474	0.0333
Reflections with [<i>I</i> > 2 σ (<i>I</i>)]	7653	9227	8458
Flack value	0.13(3)		
Parameters	542	959	512
<i>R</i> ₁ [<i>I</i> > 2 σ (<i>I</i>)]	0.0419	0.0496	0.0479
<i>wR</i> ₂ (all data)	0.0812	0.0955	0.1171
Goodness-of-fit on <i>F</i> ²	1.118	1.065	1.128

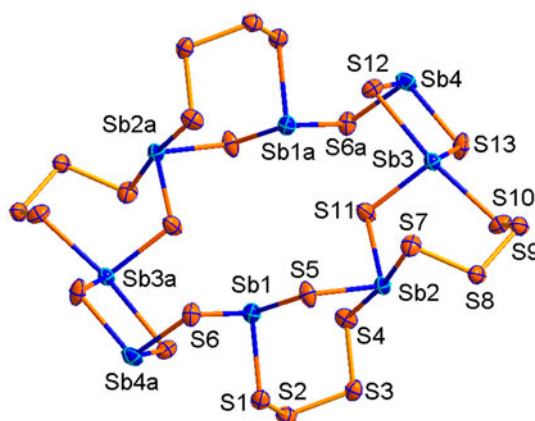
X-ray diffraction data, (figures S4, S5, and S7 in SI). The different polarity and dissolving capacity of the solvents might be attributed to formation of three thioantimonate compounds. The influence of reaction solvents on the solvothermal syntheses are also observed in syntheses of TM-containing chalcogenidoarsenates and chalcogenidostannates. The solvothermal reactions of CoCl₂, As₂O₃ and Se in H₂O and CH₃OH aqueous solution gave selenidoarsenate [Co(phen)₃]₂[As₈Se₁₄] and polyselenidoarsenate [Co(phen)₃][As₂Se₂(μ -Se₃)(μ -Se₅)], respectively [13(a)]. The selenidostannates {[Mn(phen)₂]₂(μ -Sn₂Se₆)}·H₂O, {[Mn(phen)₂](μ -Sn₂Se₆)_n}, and {[Mn(phen)₂](Sn₂Se₅)_n} with different structures were synthesized in methylamine aqueous solutions with different concentrations [21].

3.2. Crystal structures

Compound **1** crystallizes in the triclinic crystal system and contains two formula units in the unit cell (table 1). It contains one crystallographically independent Co, four Sb, and thirteen S atoms. The Co²⁺ is coordinated by three phen ligands (figure S8), forming a distorted octahedral complex [Co(phen)₃]²⁺ with Co–N distances of 2.068(4)–2.120(4) Å, and equatorial and axial N–Co–N angles of 78.99(17)–97.84(17)° and 166.26(17)–172.95(16)° (table 2), respectively. The bond lengths and angles are consistent with those of reported cobalt(II)-phen complexes [22]. As shown in figure 1, Sb(2) is equally connected with Sb (1) and Sb(3) via μ -S²⁻ and μ -S₄²⁻ bridges, forming a Sb₃S₂(S₄)₂ fragment. The Sb₃S₂(S₄)₂ fragment is shared with the Sb(4)S₃ trigonal pyramid at Sb(3) to form the asymmetric Sb₄S₅(S₄)₂ unit (figure 1). Two Sb₄S₅(S₄)₂ units are joined end-to-end via a vertex-shared sulfur (S6) to form the circular polysulfide [Sb₈S₁₀(S₄)₄]⁴⁻ anion containing a

Table 2. Selected bond lengths (Å) and angles (°) for 1–3.

	1	2	3
Sb–S ^a	2.4378(16)–2.7477(16)	2.408(6)–2.858(5)	2.317(4)–2.341(4)
Sb–S ^b	2.3701(17)–2.5044(17)	2.358(5)–2.544(4)	
S–S	2.046(2)–2.059(2)		
Co–N	2.068(4)–2.120(4)	2.052(16)–2.122(16)	2.079(8)–2.118(8)
S–Sb–S ^a	79.21(6)–173.62(5)	87.72(14)–174.02(14)	107.30(14)–111.24(14)
S–Sb–S ^b	85.76(5)–100.01(6)	87.04(17)–102.30(18)	
S–S–S	104.01(9)–107.18(10)		
Sb–S–Sb	89.35(5)–104.42(6)	89.00(17)–106.55(17)	
<i>cis</i> -N–Co–N	78.99(17)–97.84(17)	79.0(6)–95.7(6)	79.1(3)–95.4(3)
<i>trans</i> -N–Co–N	166.24(18)–172.96(17)	169.5(6)–172.5(5)	168.2(3)–171.4(3)

^aBond lengths and angles for SbS₄ units.^bBond lengths and angles for SbS₃ units.Figure 1. Crystal structure of the circular $[\text{Sb}_8\text{S}_{10}(\text{S}_4)_4]^{4-}$ anion in **1** with the labeling scheme (thermal ellipsoids are shown at 50% probability).

centrosymmetric sixteen-membered Sb_8S_8 heteroring. Among the four crystallographically independent Sb atoms, Sb(1), and Sb(4) are coordinated to three sulfides in typical SbS_3 trigonal pyramidal geometry with S–Sb–S angles of 85.76(5)–100.01(6)° and Sb–S bond lengths of 2.3701(17)–2.5044(17) Å (table 2). The Sb(2) and Sb(3) form ψ - SbS_4 trigonal bipyramids with the axial S(4)–Sb(2)–S(7) bond angles of 173.62(5)° in ψ -Sb(2)S₄ and S(10)–Sb(3)–S(12) of 163.67(5)° in ψ -Sb(3)S₄. The bond lengths of ψ - SbS_4 are 2.4378(16)–2.7477(16) Å, which are, as expected, longer than those of the SbS_3 unit. The bond lengths and angles of the SbS_3 and ψ - SbS_4 units are consistent with the corresponding values reported in the thioantimonates containing both SbS_3 and ψ - SbS_4 units [3(e), 4(d), 4(e)]. The S_4^{2-} chains possess typical S–S single-bond distances (2.046(2)–2.059(2) Å) and angles (104.01(9)–107.18(10)°) (table 2), which is in the range of corresponding values observed, such as 2.039(9)–2.069(9) Å for S–S in $\text{Cs}_5\text{Sb}_8\text{S}_{18}(\text{HCO}_3)$ [23(a)] and 2.089(5) Å for S–S in $\{(\text{C}_3\text{H}_{13}\text{N}_2)[\text{Sb}_8\text{S}_{14}]_n\}$ [23(g)]. Sb(1), and Sb(3) have additional secondary Sb⋯S interactions with S(4) and S(7) of S_4^{2-} units at distances 3.158 and 3.777 Å, respectively, (figure S9 in Supporting Information). These separations are shorter than the sum of the van der Waals radii of Sb and S (3.80 Å) [24]. Taking into account these secondary bonds

the resulting $\text{Sb}(1)\text{S}_4$ and $\text{Sb}(3)\text{S}_5$ polyhedra may be described as distorted ψ - SbS_4 trigonal bipyramid and ψ - SbS_5 octahedron, respectively.

Each $[\text{Sb}_8\text{S}_{10}(\text{S}_4)_4]^{4-}$ anion contacts with four neighbors via weak $\text{S}\cdots\text{S}$ interactions through S(6), S(9), and S(13). The $\text{S}\cdots\text{S}$ distances are 4.007 Å for S(6) \cdots S(13a) and 3.908 Å for S(9) \cdots S(9b) (figure 2), which lie in the range of 3.85–4.29 Å for $\text{S}\cdots\text{S}$ distances reported [25]. The circular $[\text{Sb}_8\text{S}_{10}(\text{S}_4)_4]^{4-}$ are interconnected by $\text{S}\cdots\text{S}$ van der Waals interactions into a 2-D layer perpendicular to the *a* axis (figure 2). The layers are parallel and the $[\text{Co}(\text{phen})_3]^{2+}$ cations are located between the layers [figure 3(a)]. Each $[\text{Co}(\text{phen})_3]^{2+}$ cation interacts with two neighbors through face-to-face $\pi\cdots\pi$ [$\pi\cdots\pi = 3.195$ and 3.333 Å] stacking interactions between the aromatic rings of phen to form zig-zag chains between the anionic layers [figure 3(b)]. The interplane $\pi\cdots\pi$ distances are in the range of those reported [22(b), 26]. The $[\text{Co}(\text{phen})_3]^{2+}$ cations interact with the anionic layers *via* weak $\text{C}\cdots\text{H}\cdots\text{S}$ hydrogen bonds with $\text{H}\cdots\text{S}$ distances from 2.802–2.928 Å. A large number of TM complexes containing thioantimonates have been prepared by solvothermal methods in polyamine solution [3–12]. However, no polythioantimonates are observed in these compounds. Compound **1** is the first example of polysulfido-thioantimonate prepared by solvothermal method using a TM complex as structure directing agent, although a number of polysulfido-polythioantimonates had been obtained in aqueous ammonia solutions or by flux methods [23].

Compound **2** is isostructural to the Ni-analog $[\text{Ni}(\text{phen})_3]_2\text{Sb}_{18}\text{S}_{29}$ [15(a)]. It contains two crystallographically independent Co ions, eighteen Sb, and twenty-nine sulfurs. Both Co^{2+} ions are coordinated by three phen ligands, forming $[\text{Co}(\text{phen})_3]^{2+}$ (figure S10 [see online supplemental material at <http://dx.doi.org/10.1080/00958972.2015.1045500>]), similar to the $[\text{Co}(\text{phen})_3]^{2+}$ cation in **1** (table 2). With the exception of Sb(7) and Sb(8), each Sb is coordinated to three sulfurs at distances of 2.358(5)–2.544(4) Å in approximately trigonal pyramidal geometry with S–Sb–S angles of 87.04(17)–102.30(18)° (table 2). Sb(7) and Sb(8) are coordinated to four sulfurs, forming the so-called ψ - SbS_4 trigonal bipyramids with two short (Sb–S: 2.408(6)–2.485(5) Å) and two longer (Sb–S: 2.618(4)–2.858(5) Å) Sb–S bonds. Within the ψ - SbS_4 trigonal bipyramids, the axial S–Sb–S bond angles are 173.76

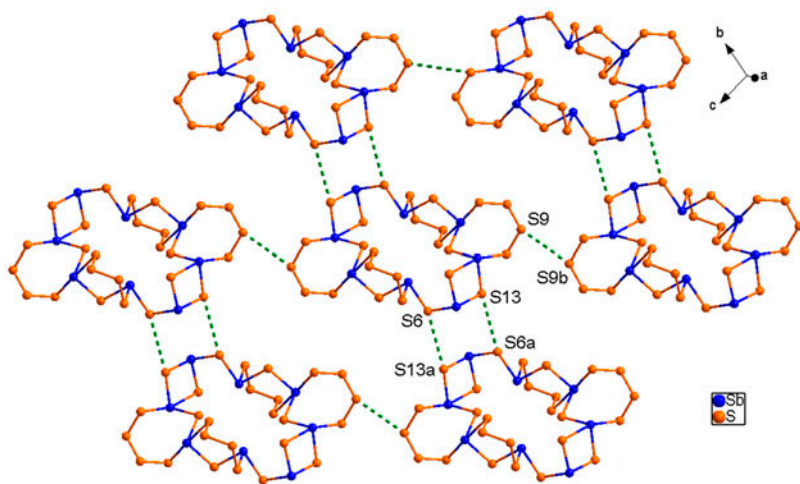


Figure 2. A layer of the $[\text{Sb}_8\text{S}_{10}(\text{S}_4)_4]^{4-}$ anions assembled through $\text{S}\cdots\text{S}$ interactions in **1**.

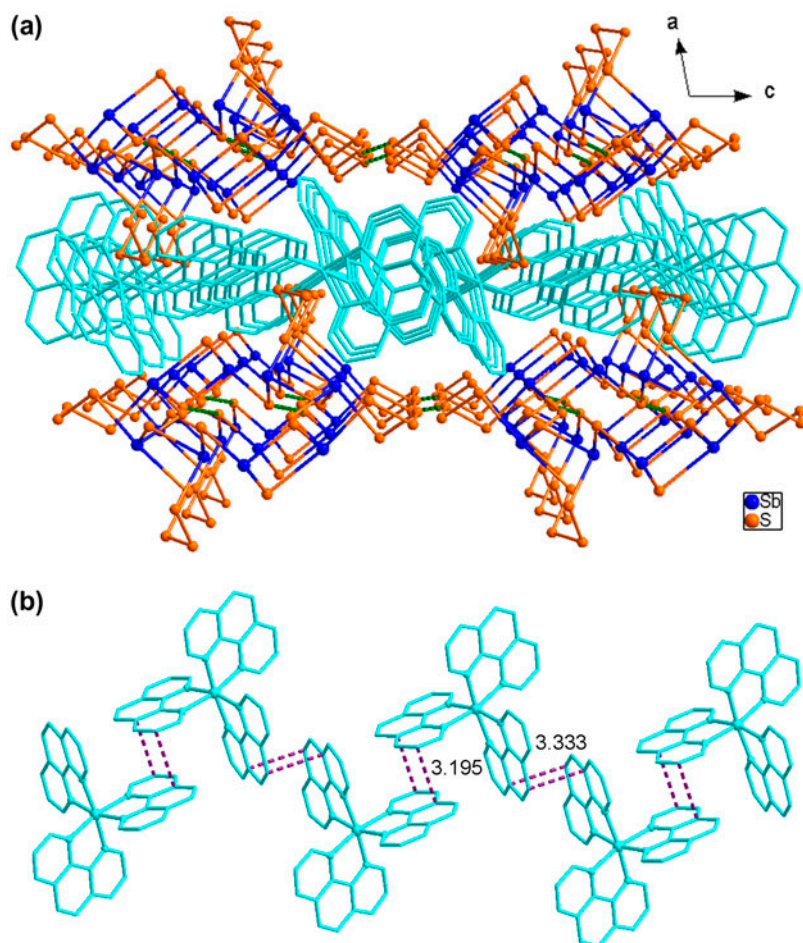


Figure 3. (a) Packing diagram of **1** viewed down the crystallographic b axis. (b) A view of the zig-zag chain of $[\text{Co}(\text{phen})_3]^{2+}$ cations assembled by face-to-face $\pi \cdots \pi$ stacking interactions in **1**. Hydrogens are omitted for clarity.

(15° and $174.02(14)^\circ$, the equatorial S–Sb–S bond angles are $95.41(17)^\circ$ and $95.64(18)^\circ$, and the bond angles between apical and equatorial sulfurs range from $87.72(14)$ to $93.19(15)^\circ$. The bond lengths and angles of the SbS_3 and $\psi\text{-SbS}_4$ units are consistent with the corresponding values in **1** (table 2, tables S1 and S2). The sixteen SbS_3 trigonal pyramids and two $\psi\text{-SbS}_4$ trigonal bipyramids are interconnected by sharing S to form the asymmetric $\text{Sb}_{18}\text{S}_{29}$ unit, in which Sb_9S_9 , Sb_8S_8 , and Sb_7S_7 heterorings are formed (figure S11). Excepting terminal sulfurs S(6) and S(29), twenty-seven of the twenty-nine crystallographically independent sulfurs are $\mu\text{-S}$ ligands to join two Sb with Sb–S–Sb angles of $89.00(17)$ – $106.55(17)^\circ$ (table 2). All antimony atoms with the exception of Sb(18) have additional sulfur neighbors at longer distances of 2.940 – 3.743 Å, which are less than the sum of van der Waals' radii (3.80 Å) of antimony and sulfur [24].

Each asymmetric $\text{Sb}_{18}\text{S}_{29}$ unit is further joined to four neighbors *via* five bridges, $\mu\text{-S}(3)$, $\mu\text{-S}(12)$, $\mu\text{-S}(20)$, $\mu\text{-S}(21)$, and $\mu\text{-S}(23)$, in three dimensions to generate the full 3-D

structure of $[\text{Sb}_{18}\text{S}_{29}^{4-}]_{\infty}$ [figure 4(a)]. These connections give rise to $\text{Sb}_{22}\text{S}_{22}$ and $\text{Sb}_{18}\text{S}_{18}$ large heterorings. $\text{Sb}_{22}\text{S}_{22}$ is formed by twenty SbS_3 pyramids and two SbS_4 units *via* sharing common corners [figure 4(b)], while $\text{Sb}_{18}\text{S}_{18}$ is formed by eighteen SbS_3 pyramids sharing common corners [figure 4(d)]. This 3-D structure contains two intersecting channels, one running along the a axis, as a consequence of the stacking of the $\text{Sb}_{22}\text{S}_{22}$ rings, and the other along the c axis, as a consequence of the stacking of the $\text{Sb}_{18}\text{S}_{18}$ rings (figure S12). The channel along the a axis has a square cross section of ca. $10.38 \times 20.25 \text{ \AA}$ and the $[\text{Co}(\text{phen})_3]^{2+}$ cations are located in this channel. As shown in figure 4(a), each channel along the a axis encloses two parallel arrays of $[\text{Co}(\text{phen})_3]^{2+}$ cations which are composed of $[\text{Co}(1)(\text{phen})_3]^{2+}$ and $[\text{Co}(2)(\text{phen})_3]^{2+}$, respectively. The aromatic plane of one phen in $[\text{Co}(1)(\text{phen})_3]^{2+}$ (that containing N1 and N2) is parallel to that of a phen ligand in neighboring $[\text{Co}(2)(\text{phen})_3]^{2+}$ (that containing N11 and N12). The interplane distance between the centroids of the two phen ligands is 3.409–3.497 \AA , indicating weak intermolecular $\pi \cdots \pi$ stacking interactions [figure 4(c)]. These face-to-face $\pi \cdots \pi$ stacking interactions arrange $[\text{Co}(1)(\text{phen})_3]^{2+}$ and $[\text{Co}(2)(\text{phen})_3]^{2+}$ cations in parallel arrays along the channel in the 3-D $[\text{Sb}_{18}\text{S}_{29}^{4-}]_{\infty}$ framework.

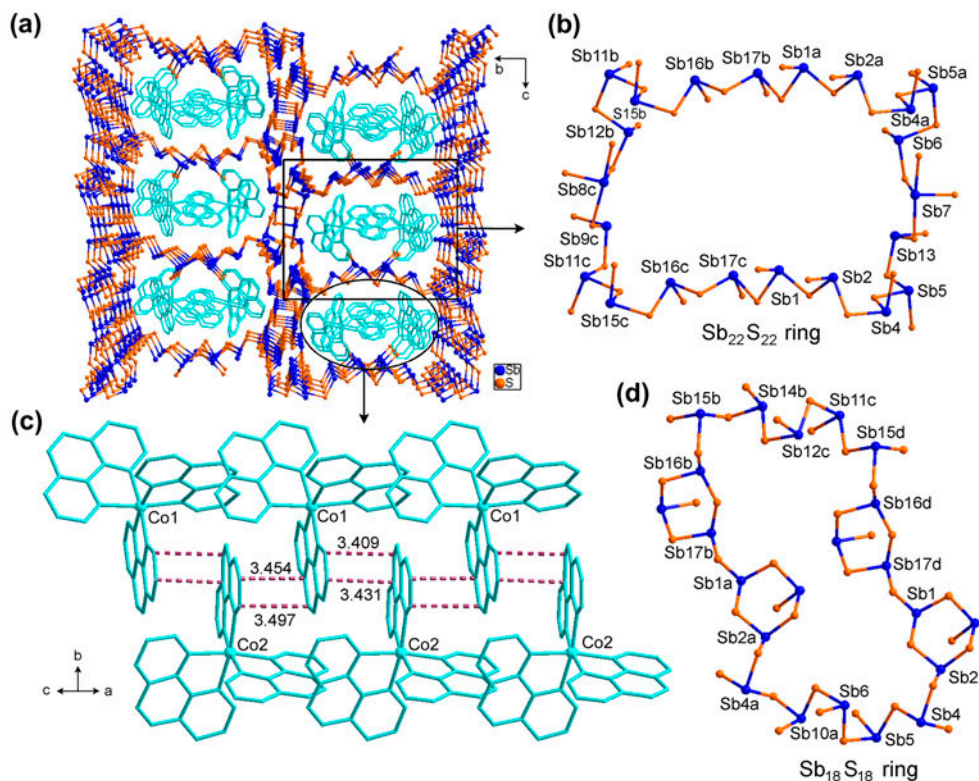


Figure 4. (a) Packing diagram of **2** viewed down the crystallographic a axis, showing the 1-D channels in the 3-D $[\text{Sb}_{18}\text{S}_{29}^{4-}]_{\infty}$ framework. (b) A view of the cross section of the 1-D channels along the a axis in **2**. (c) A view of the double parallel arrays of the $[\text{Co}(\text{phen})_3]^{2+}$ cations assembled by face-to-face $\pi \cdots \pi$ stacking interactions in **2**. (d) A view of the cross section of the 1-D channels along the c axis in **2**. Hydrogens are omitted for clarity.

Compound **3** crystallizes in the triclinic crystal system and contains two formula units in the unit cell. It consists of a $[\text{Co}(\text{phen})_3]^{2+}$, a $[\text{SbS}_4]^{3-}$ anion, a protonated H_2O , and nine lattice water molecules. The $[\text{Co}(\text{phen})_3]^{2+}$ has a similar structure to the complex cations in **1** and **2** (table 2). The Sb^{5+} is coordinated by four S^{2-} to form a tetrahedral $[\text{SbS}_4]^{3-}$ anion with S–Sb–S angles of $107.30(14)$ – $111.24(14)^\circ$. The Sb–S bond lengths ($2.317(4)$ – $2.341(4)$ Å) are shorter than those of $\text{Sb}^{\text{III}}\text{S}_3$ unit observed in **1** and **2** (table 2). The interesting structural feature of **3** is the existence of water clusters. The $[\text{SbS}_4]^{3-}$ contacts a H_3O^+ and six H_2O molecules (O1, O3, O6, O7, O9, O10) via O–H \cdots S intermolecular hydrogen bonds [$\text{O}\cdots\text{S} = 3.154(16)$ – $3.79(3)$ Å], forming a $\{\text{H}_3\text{O}-\text{SbS}_4-(\text{H}_2\text{O})_6\}^{2-}$ unit (figure 5). All the S atoms of $[\text{SbS}_4]^{3-}$ are involved in hydrogen bonds with water molecules. The $\{\text{H}_3\text{O}-\text{SbS}_4-(\text{H}_2\text{O})_6\}^{2-}$ unit and the rest of the H_2O molecules are interconnected via O–H \cdots O [$\text{O}\cdots\text{O} = 2.44(4)$ – $2.948(19)$ Å] hydrogen bonds into a $\{\text{H}_3\text{O}-\text{SbS}_4-(\text{H}_2\text{O}_9)\}_n^{2n-}$ anionic layer [figure 6(a)]. In the layer, a $(\text{H}_2\text{O})_6$ water cluster is observed. $[\text{Co}(\text{phen})_3]^{2+}$ cations are embedded between the anionic layers [figure 6(b)]. Water clusters or infinite water chains and layers have drawn attention, and a number of water clusters, chains, and layers have been structurally characterized in metal complexes. These water clusters are usually stabilized by O–H \cdots O and/or O–H \cdots N interactions between water molecules and O or N in the organic or inorganic host [27]. However, the water clusters hosted in the chalcogenometalate compounds and stabilized by weak O–H \cdots S interactions are very rare. We have once obtained the first water chain in the thioarsenate $[\text{Fe}(\text{phen})_3][\text{As}_3\text{S}_6]\cdot\text{dien}\cdot 7\text{H}_2\text{O}$. The water chain is anchored on the $[\text{As}_3\text{S}_6]^{3-}$ anions via O–H \cdots S hydrogen bonding interactions, forming a $\{\text{As}_3\text{S}_6-(\text{H}_2\text{O})_7\}_n^{3n-}$ layer [26]. The thioantimonate-water layer $\{\text{H}_3\text{O}-\text{SbS}_4-(\text{H}_2\text{O}_9)\}_n^{2n-}$ in **3** has never been observed in chalcogenidoantimonates before.

3.3. Optical properties

The UV–vis reflectance spectroscopic measurement of **1–3** was recorded using powder samples at room temperature. Absorption data from the reflectance spectroscopy by the Kubelka-Munk function [17] demonstrate that **1–3** exhibit steep absorption edges with corresponding band gaps (E_g) of 2.04, 2.11 and 2.27 eV, respectively (figure 7). This indicates these compounds exhibit possible semiconducting properties. The band gap of **2** is

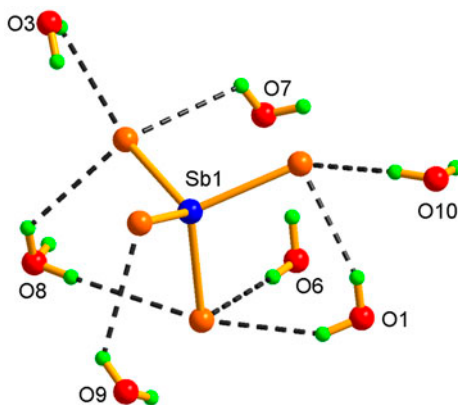


Figure 5. Intermolecular O–H \cdots S interactions between $[\text{SbS}_4]^{3-}$ and H_3O^+ , and H_2O in **3**.

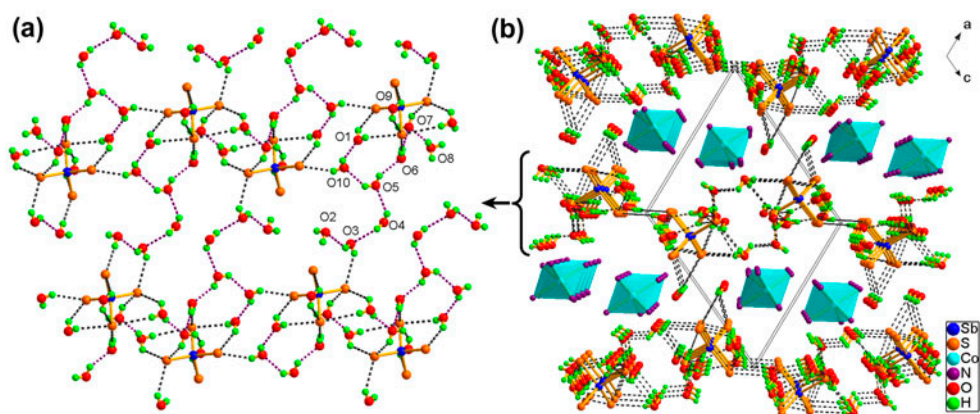


Figure 6. (a) A view of the $\{\text{H}_3\text{O-SbS}_4\text{-(H}_2\text{O}_9)\}_n^{2n-}$ H-bonding layer in **3**. (b) Packing diagram of **3** viewed down the crystallographic *b* axis, showing the $[\text{Co}(\text{phen})_3]^{2+}$ cations sandwiched between the $\{\text{H}_3\text{O-SbS}_4\text{-(H}_2\text{O}_9)\}_n^{2n-}$ layers. C and H are omitted for clarity. Cyan octahedron: CoN_6 .

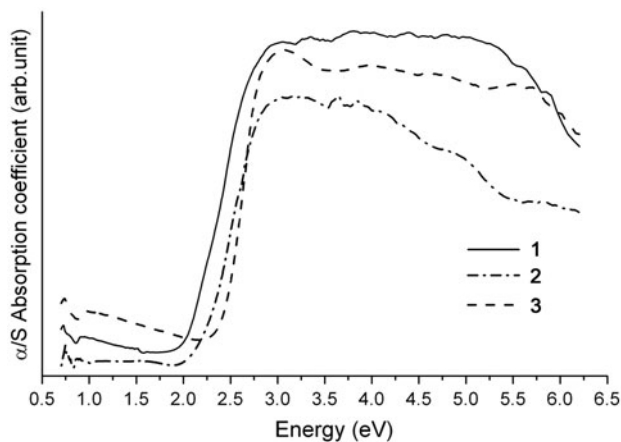


Figure 7. Solid state optical absorption spectra of **1–3**.

comparable to the Ni-analog ($E_g = 2.16$ eV) [15(a)]. The band gap of **1** and **2** are smaller than those of Co-thioantimonates(III) containing aliphatic polyamine ligands, such as $[\text{Co}(\text{en})_3]\text{Sb}_2\text{S}_4$ ($E_g = 2.52$ eV) [3(c)] and $[\text{Co}(\text{tren})]\text{Sb}_4\text{S}_7$ ($E_g = 2.45$ eV) [5(e)]. Blue shift of the absorption edge is observed from Co-complexes of aromatic ligands to the Co-complexes of aliphatic ligands.

4. Conclusion

Solvent effects on the solvothermal system Co/Sb/S/phen have been observed, and polysulfido-thioantimonate and thioantimonates **1–3** were prepared in mixed $\text{CH}_3\text{OH-H}_2\text{O}$ and

H₂O solvents, respectively. S₈ is converted to both polysulfide anion S₄²⁻ and sulfide anion S²⁻ in 80% CH₃OH aqueous solvent, while it is converted to sulfide S²⁻ in 50% CH₃OH and H₂O solvents. Compound **1** contains a circular anion [Sb₈S₁₀(S₄)₄]⁴⁻ constructed by both sulfide and polysulfide ions. The 3-D [Sb₁₈S₂₉]⁴⁻∞ framework in **2** possesses an interpenetrating channel system and the [Co(phen)₃]²⁺ complexes are enclosed in the channels. Compound **3** contains a water cluster stabilized by O–H···S and O–H···O hydrogen bonding interactions. The solvent effects on the TM/Sb/S/phen system of other TMs are under investigation.

Supplementary material

Crystallographic data for the structures reported in the article have been deposited at the Cambridge Crystallographic Data Center as supplementary data, CCDC Nos. 1018727 (**1**), 1018728 (**2**), and 1018751 (**3**). Copies of the data can be obtained free of charge via www.ccdc.cam.ac.uk/conts/retrieving.html or from the Cambridge Crystallographic Data Center, 12 Union Road, Cambridge CB2 1EZ, UK; Fax: (+44) 1223 336 033, or E-mail: deposit@ccdc.cam.ac.uk.

Disclosure statement

No potential conflict of interest was reported by the authors.

References

- [1] (a) W.S. Sheldrick, M. Wachhold. *Coord. Chem. Rev.*, **176**, 211 (1998); (b) J. Li, Z. Chen, R.J. Wang, D.M. Proserpio. *Coord. Chem. Rev.*, **190–192**, 707 (1999); (c) S. Dehnen, M. Melullis. *Coord. Chem. Rev.*, **251**, 1259 (2007); (d) B. Seidlhofer, N. Pienack, W. Bensch. *Z. Naturforsch.*, **65b**, 937 (2010).
- [2] (a) H.O. Stephan, M.G. Kanatzidis. *J. Am. Chem. Soc.*, **118**, 12226 (1996); (b) K.S. Choi, M.G. Kanatzidis. *Chem. Mater.*, **11**, 2613 (1999); (c) K.S. Choi, J.A. Hanko, M.G. Kanatzidis. *J. Solid State Chem.*, **147**, 309 (1999); (d) K.S. Choi, M.G. Kanatzidis. *Chem. Mater.*, **39**, 5655 (2000).
- [3] (a) W. Bensch, M. Schur. *Z. Naturforsch.*, **52b**, 405 (1997); (b) M. Schur, W. Bensch. *Z. Naturforsch.*, **57b**, 1 (2001); (c) H.O. Stephan, M.G. Kanatzidis. *Inorg. Chem.*, **36**, 6050 (1997); (d) P. Vaqueiro, D.P. Darlow, A.V. Powell, A.M. Chippindale. *Solid State Ionics*, **172**, 601 (2004); (e) P. Vaqueiro, A.M. Chippindale, A.V. Powell. *Inorg. Chem.*, **43**, 7963 (2004).
- [4] (a) R. Stähler, W. Bensch. *Acta Cryst.*, **C57**, 26 (2001); (b) R. Stähler, W. Bensch. *Z. Anorg. Allg. Chem.*, **628**, 1657 (2002); (c) W. Bensch, C. Näther, R. Stähler. *Chem. Commun.*, 477 (2001); (d) R. Stähler, B.D. Mosel, H. Eckert, W. Bensch. *Angew. Chem. Int. Ed.*, **41**, 4487 (2002); (e) R. Stähler, C. Näther, W. Bensch. *J. Solid State Chem.*, **174**, 264 (2003); (f) R. Kiebach, F. Studt, C. Näther, W. Bensch. *Eur. J. Inorg. Chem.*, 2553 (2004); (g) R. Stähler, C. Näther, W. Bensch. *Eur. J. Inorg. Chem.*, 1835 (2001); (h) M. Zhang, T.L. Sheng, X. Wang, S.M. Hu, R.B. Fu, J.S. Chen, Y.M. He, Z.T. Qin, C.J. Shen, X.T. Wu. *CrystEngChem.*, **12**, 73 (2010).
- [5] (a) R. Stähler, W. Bensch. *Eur. J. Inorg. Chem.*, 3073 (2001); (b) M. Schaefer, C. Näther, W. Bensch. *Solid State Sci.*, **5**, 1135 (2003); (c) R. Kiebach, W. Bensch, R.D. Hoffmann, R. Pöttgen. *Z. Anorg. Allg. Chem.*, **629**, 532 (2003); (d) M. Schaefer, C. Näther, N. Lehnert, W. Bensch. *Inorg. Chem.*, **43**, 2914 (2004); (e) M. Schaefer, R. Stähler, W.R. Kiebach, C. Näther, W. Bensch. *Z. Anorg. Allg. Chem.*, **630**, 1816 (2004); (f) M. Schaefer, D. Kurowski, A. Pfitzner, C. Näther, Z. Rejai, K. Möller, N. Ziegler, W. Bensch. *Inorg. Chem.*, **45**, 3726 (2006); (g) J. Lichte, H. Lühmann, C. Näther, W. Bensch. *Z. Anorg. Allg. Chem.*, **635**, 2021 (2009).
- [6] (a) H. Lühmann, Z. Rejai, K. Möller, P. Leisner, M.E. Ordoñf, C. Näther, W. Bensch. *Z. Anorg. Allg. Chem.*, **634**, 1687 (2008); (b) Z. Rejai, H. Lühmann, C. Näther, R.K. Kremer, W. Bensch. *Inorg. Chem.*, **49**, 1651 (2010).

- [7] (a) L. Engelke, C. Näther, P. Leisner, W. Bensch. *Z. Anorg. Allg. Chem.*, **634**, 2959 (2008); (b) H. Lühmann, C. Näther, W. Bensch. *Z. Anorg. Allg. Chem.*, **637**, 1007 (2011); (c) B. Seidlhofer, C. Näther, W. Bensch. *CrystEngComm*, **14**, 5441 (2012).
- [8] (a) V. Spetzler, H. Rijnberk, C. Näther, W. Bensch. *Z. Anorg. Allg. Chem.*, **630**, 142 (2004); (b) V. Spetzler, C. Näther, W. Bensch. *Inorg. Chem.*, **44**, 5805 (2005); (c) A.V. Powell, R. Paniagua, P. Vaqueiro, A.M. Chippindale. *Chem. Mater.*, **14**, 1220 (2002).
- [9] (a) P. Vaqueiro, A.M. Chippindale, A.R. Cowley, A.V. Powell. *Inorg. Chem.*, **42**, 7846 (2003); (b) A.V. Powell, J. Thum, A.M. Chippindale. *J. Solid State Chem.*, **178**, 3414 (2005); (c) V. Spetzler, C. Näther, W. Bensch. *J. Solid State Chem.*, **179**, 3541 (2006).
- [10] M. Schur, H. Rijnberk, C. Näther, W. Bensch. *Polyhedron*, **18**, 101 (1998).
- [11] M. Schaefer, L. Engelke, W. Bensch. *Z. Anorg. Allg. Chem.*, **629**, 1912 (2003).
- [12] M. Schur, W. Bensch. *Acta Cryst.*, **C56**, 1107 (2000).
- [13] (a) Y.L. Pan, J.F. Chen, J. Wang, Y. Zhang, D.X. Jia. *Inorg. Chem. Commun.*, **13**, 1569 (2010); (b) W.W. Tang, R.H. Chen, J. Zhao, W.Q. Jiang, Y. Zhang, D.X. Jia. *CrystEngComm*, **14**, 5021 (2012).
- [14] J. Lichte, C. Näther, W. Bensch. *Z. Anorg. Allg. Chem.*, **636**, 108 (2010).
- [15] (a) K.Z. Du, M.L. Feng, L.H. Li, B. Hu, Z.J. Ma, P. Wang, J.R. Li, Y.L. Wang, G.D. Zou, X.Y. Huang. *Inorg. Chem.*, **51**, 3926 (2012); (b) X. Wang, T.L. Sheng, S.M. Hu, R.B. Fu, X.T. Wu. *Inorg. Chem. Commun.*, **12**, 399 (2009); (c) C. Anderer, C. Näther, W. Bensch. *Inorg. Chem. Commun.*, **46**, 335 (2014).
- [16] (a) J. Zhao, J.J. Liang, J.F. Chen, Y.L. Pan, Y. Zhang, D.X. Jia. *Inorg. Chem.*, **50**, 2288 (2011); (b) D.X. Jia, J. Zhao, Y.L. Pan, W.W. Tang, B. Wu, Y. Zhang. *Inorg. Chem.*, **50**, 7195 (2011).
- [17] W.W. Wendlandt, H.G. Hecht. *Reflectance Spectroscopy*, Interscience Publishers, New York (1966).
- [18] CrystalClear. (Version 1.35), Rigaku Corp., Tokyo (2002).
- [19] G.M. Sheldrick. *SHELXS-97; Program for Crystal Structure Determination*, University of Göttingen, Göttingen (1997).
- [20] G.M. Sheldrick. *SHELXL-97; Program for the Refinement of Crystal Structures*, University of Göttingen, Göttingen (1997).
- [21] G.N. Liu, G.C. Guo, M.J. Zhang, J.S. Guo, H.Y. Zeng, J.S. Huang. *Inorg. Chem.*, **50**, 9660 (2011).
- [22] (a) C.M. Liu, D.Q. Zhang, D.B. Zhu. *Cryst. Growth Des.*, **3**, 363 (2003); (b) F. Gándara, C. Fortes-Revilla, N. Sneško, E. Gutiérrez-Puebla, M. Iglesias, M.A. Monge. *Inorg. Chem.*, **45**, 9680 (2006).
- [23] (a) G.L. Schimek, J.W. Kolis. *Inorg. Chem.*, **36**, 1689 (1997); (b) M. Schur, W. Bensch. *Z. Anorg. Allg. Chem.*, **624**, 310 (1998); (c) W. Bensch, M. Schur. *Z. Kristallogr. New Cryst. Struct.*, **212**, 305 (1997); (d) H. Rijnberk, C. Näther, M. Schur, I. Jeß. *Acta Cryst.*, **C54**, 920 (1998); (e) R.G. Iyer, M.G. Kanatzidis. *Inorg. Chem.*, **41**, 3605 (2002); (f) R.J.E. Lees, A.V. Powell, A.M. Chippindale. *Acta Cryst.*, **C61**, m516 (2005); (g) A. Puls, C. Näther, W. Bensch. *Acta Cryst.*, **E62**, m1045 (2006).
- [24] A. Bondi. *J. Phys. Chem.*, **68**, 441 (1964).
- [25] (a) P. Hudhomme, S. Le Moustarder, C. Durand, N. Gallego-Planas, N. Mercier, P. Blanchard, E. Levillain, M. Allain, A. Gorgues, A. Riou. *Chem. Eur. J.*, **7**, 5070 (2001); (b) K. Kobayashi, R. Shimaoka, M. Kawahata, M. Yamanaka, K. Yamaguchi. *Org. Lett.*, **8**, 2385 (2006); (c) M. Arooj, K.H. Kim, D.H. Kim, B.S. Kim, G.Y. Park, S.H. Jeong, S.C. Shin, J.K. Park. *Bull. Korean Chem. Soc.*, **30**, 3079 (2009).
- [26] Y.L. Pan, Q.Y. Jin, J.F. Chen, Y. Zhang, D.X. Jia. *Inorg. Chem.*, **48**, 5412 (2009).
- [27] (a) L.E. Cheruzel, M.S. Pometun, M.R. Cecil, M.S. Mashuta, R.J. Wittebort, R.M. Buchanan. *Angew. Chem., Int. Ed.*, **42**, 5452 (2003); (b) P.S. Lakshminarayanan, E. Suresh, P. Ghosh. *J. Am. Chem. Soc.*, **127**, 13132 (2005); (c) B.K. Saha, A. Nangia. *Chem. Commun.*, 1825 (2006); (d) C. Biswas, M.G.B. Drew, A. Ghosh. *Inorg. Chem.*, **47**, 4513 (2008); (e) S.Q. Bai, T.S. Andy. *Hor. Chem. Commun.*, 3172 (2008).